Dynamic Light Scattering and Dynamic Viscoelasticity of Poly(vinyl alcohol) in Aqueous Borax Solutions. 4. Further Investigation on Polymer Concentration and Molecular Weight Dependencies†

Akihiko Takada,* Miki Nishimura,‡ Akihiro Koike,§ and Norio Nemoto

Department of Applied Physics, Faculty of Engineering, Kyushu University, Hakozaki, Fukuoka 812-81, Japan

Received June 12, 1997[⊗]

ABSTRACT: Viscosity measurements are made on aqueous borax solutions of poly(vinyl alcohol) (PVA) samples over a wide range of PVA concentration, C, to examine the hydrodynamic properties of associated polymers compared to those of neutral polymers. The dynamic viscoelastic data are reanalyzed using a statistical−mechanical theory for elastically effective chains in transient gels developed by Tanaka and Ishida. The viscosity data are not superposed in the plot of viscosity against $C[\eta]$ using the Huggins relationship, especially around and over a critical concentration, C_N, at which the dynamical behaviors drastically change and an inflection point of a curve in the plot of the viscosity against C is located. On the other hand, when we assume that the chain dimension around C_N is the unperturbed one, the viscosity data around C_N is well-superposed on a curve in the plot of viscosity against C/C^*_{up}, where C^*_{up} is the overlapping concentration of the unperturbed chain. The inflection point of this composite curve is located at $C/C^*_{up} = 1$, which infers that C_N corresponds to the overlapping concentration. All data of the density of elastically effective chains, ν_{eff}, are superposed on a curve in the plot of ν_{eff}/ν against $(C - C_N)/C_N$ where ν is the density of polymer chains, which implies that C_N should be regarded as a kind of gel point. Some discrepancies between the experimental data and the theoretical curve were observed, some of which cannot be explained using the pairwise association of PVA chains.

Introduction

In previous reports,[1−3] we studied the dynamics of poly(vinyl alcohol) in aqueous borax solutions (PVA/SB) as functions of polymer concentration, C, and molecular weight, M (or the degree of polymerization, DP), using dynamic light scattering (DLS) and dynamic viscoelastic (DVE) methods. A characteristic feature of this system was found to be the presence of the critical concentration, C_N, at which drastic changes in the dynamical behavior took place. We interpreted C_N as the concentration at which clusters growing with an increase in C were combined to form a viscoelastic network uniform over the whole sample volume with a didiol complex as temporal cross-link.

The scaling concept developed by de Gennes[4] gives such a simple picture that flexible polymer solution without any specific intermolecular interaction should abruptly change their static and dynamical properties at the overlapping concentration C^* accompanied by the transition from the dilute regime to the semidilute regime. The characteristic length scale in the former regime is the radius of gyration, R_G, or the hydrodynamic radius, R_H, of the isolated polymer molecule, while it is replaced by the static (or dynamical) correlation length, ξ_s (or ξ_H), in the latter regime. On the basis of the finding that the values of C_N are close to values of C^* calculated from the intrinsic viscosity, $[\eta]$, of PVA in pure aqueous solution in literature[5] with the conventional relation $C^* = 1/[\eta]$, we inferred that chain overlapping also played an important role for network formation of the PVA/SB system. For $C > C_N$, dynamics of the network was described in terms of the only length, ξ_H, dependent on C as expected. For $C < C_N$, however, the system possessed two characteristic lengths, one being the cluster size, R_s, and another ξ_H, which was dependent on DP but independent of C. This suggests that the simple argument using the scaling theory would not be applicable. At any rate, comparison of C_N with C^* should be made, at least, using $[\eta]$ values of PVA measured in aqueous borax solution, and a difference in hydrodynamic properties between neutral polymer and associating polymers will be disclosed by viscosity measurements over the wide C range up to C_N.

Cross-links composed of the ionic didiol complex for the PVA/SB system have a finite lifetime, so the network behaves as viscous liquid at long times, and its dynamic viscoelasticity in the low angular frequency (ω) region may be characterized by the terminal relaxation time (τ_m) and the steady flow viscosity (η). On the other hand, dynamic viscoelastic measurements on the samples with $C > C_N$ revealed that the ω dependence of storage shear modulus, $G'(\omega)$, took plateau with the value (plateau modulus) G_N at high ω values, which may offer another interpretation of C_N as the sol−gel transition point in the short time domain for the PVA/SB system. In this connection, we became aware of a statistical−mechanical theory for elastically effective chains in transient gels developed by Tanaka and Ishida[6] quite recently. The network is modeled as a collection of primary flexible chains with n repeating units carrying f functional groups capable of forming multiple junctions, each of which is composed of m functional groups combining more than two network

† Part 4 of the series "Dynamic Light Scattering and Dynamic Viscoelasticity of Poly(vinyl alcohol) in Aqueous Borax Solutions".

* To whom correspondence should be addressed.

‡ Present address: Figaro Engineering Co. Ltd., Senba-nishi 1, Minou, Osaka 562, Japan.

§ Present address: Japan Synthetic Rubber Co. Ltd., Kawajiri, Yokkaichi, Mie 510, Japan.

⊗ Abstract published in *Advance ACS Abstracts,* December 15, 1997.

S0024-9297(97)00859-0 CCC: $15.00
Published on Web 01/07/1998

chains. f is proportional to the DP and m may be equal to 2 for a case of the PVA/SB system. Then, we expect that analysis of measured G_N data with the theory without any adjustable parameter will give us a more clear-cut physical meaning of C_N as well as information on the network structure. It is to be noted that C_N, though here termed as the critical concentration, is not the true critical point observed in the gelation process for a chemically cross-linked gel, which percolates and takes the self-similar structure at the critical extent of the chemical reaction. If this were the case, ω dependence of the storage and loss moduli, $G'(\omega)$ and $G''(\omega)$, of the PVA/SB system would follow the power law with the same relaxation exponent at C_N as probed by Winter and his associates and many researchers including our group.[7−10]

This paper attempts to answer the two issues raised above from viscosity measurements on aqueous borax solutions of five PVA samples with weight-average degree of polymerization (DP_w) = 350, 600, 2100, 2600, and 3250 and also from reanalysis of DVE data reported earlier, respectively. To this end, we briefly summarize earlier DLS and DVE results on the same samples which clearly exhibit the importance of C_N as a characteristic parameter in this system and whose description seems convenient for later discussion.

Experimental Section

Materials. The five poly(vinyl alcohol) (PVA) samples used in this study were a gift from Kuraray Co., Ltd. The DP_w of the samples are 350, 600, 2100, 2600, and 3250 with the molecular weight distribution of M_w/M_n = 2.60, 2.58, 2.18, 2.08, and 2.00, respectively, and with the same degree of saponification, 88.0 mol %, being characterized by the supplier. Concentrated stock solutions of PVA and of sodium borate (SB), $Na_2B_4O_7{\cdot}10H_2O$, was separately prepared using dust-free purified water and made optically clean by filtration with a Millipore filter (nominal pore size, 0.22 μm). Prescribed amounts of the two stock solutions were mixed to obtain the solution of desired polymer concentration C by weight. The SB concentration was always adjusted to be half that of PVA by weight. Finally, the cell was rotated at 0.2 rpm for about 2 h at 80 °C in order to make samples homogeneous and transparent. More than five solutions with different C values were prepared with this procedure for respective PVA samples. It became tremendously difficult to prepare homogeneous solution with C higher than that listed in the tables, especially for the highest molecular weight PVA samples. The sample code PVA X-Y given in the tables represents DP_w as X and C as Y in weight percent for the PVA/SB solutions tested.

Methods. Viscosities of dilute solutions with and without SB for five PVA samples with DP_w from 350 to 3250 was measured with an Ubbelohde type of capillary viscometer. The C range of the solutions is lower than about half the value of C_N. It is reported that semidilute PVA/SB solutions exhibit the shear-thickening phenomenon, which was revealed in steady flow measurement.[11,12] We measured viscosities of the highest C solutions measured by the capillary viscometer by use of a Cannon−Fenske type of viscometer with much lower flow rate than that obtained by the Ubbelohde type of viscometer. The viscosities were in good agreement to each other, which indicates that the values of viscosity is not affected by the shear−thickening phenomenon.

For solutions of five PVA samples, dynamic viscoelastic (DVE) measurements were made with a stress-controlled rheometer (CSL100, Carri-MED, ITS Japan) using a cone-and-plate geometry with a cone diameter of 4 cm and a cone angle of 2°. The complex modulus was found to be independent of the strain applied when the strain was less than 0.7. In this study, the storage and the loss shear moduli, $G'(\omega)$ and $G''(\omega)$, of the samples were measured at a strain of 0.3 over angular frequency, ω, from 0.07 to 100 rad/s at T = 25 °C. A humidity chamber was used to prevent solvent evaporation.

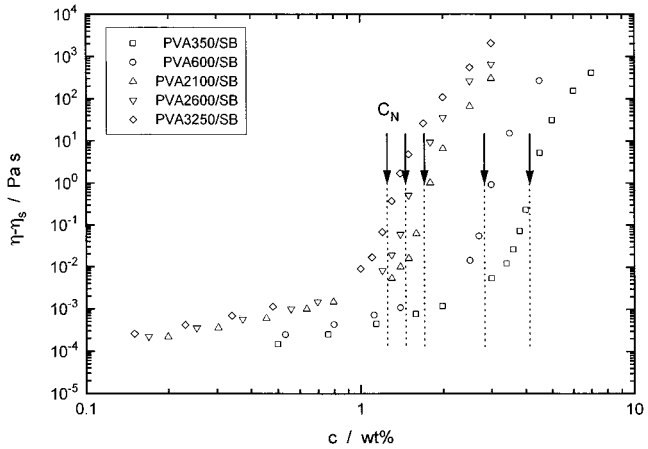

Figure 1. C dependence of $\eta - \eta_s$ for five PVA samples where η is the steady-state viscosity and η_s the solvent viscosity. An arrow indicates the inflection point in the η vs C curve and is put equal to C_N.

The steady-state shear viscosity of the solutions which possessed viscosity lower than that estimated from DVE measurements but higher than that measured by the capillary viscometer was measured with the same geometry as used for the dynamic viscoelastic measurements with a shear rate sufficiently lower than the shear rate at which shear thickening occurs.

Dynamic light scattering (DLS) measurements were made with a spectrometer (ALV-125) equipped with a multiple τ correlator (ALV-5000FAST). A vertically polarized single-frequency 488 nm line of an argon ion laser (Spectra Physics, Beamlok 2060) was used as a light source with an output power of 300 mW. The normalized time correlation function, $A_q(t)$, of the vertical component of the light intensity scattered from the solutions of PVA samples was measured over a range of the scattering angle θ from 15° to 150° at a temperature T = 25 °C.

Results

Viscosity Behavior. In Figure 1, $\eta - \eta_s$ is plotted against C, where η_s is a viscosity of pure water. The data were located on a smooth curve for a each molecular weight sample. All curves have the characteristic sigmoidal shape. Following the analysis in a previous paper,[2,3] we made C_N equal to the concentration at the inflection point. The $\eta - \eta_s$ at the inflection point takes almost a constant value around 0.1 Pa·s irrespective of the molecular weight of PVA. Figure 2 shows a logarithmic plot of C_N against DP_w and indicates that the M dependence of C_N is represented by $C_N \sim M^{-0.53\pm0.02}$, as given by a straight line in the figure.

In order to estimate the intrinsic viscosity, we plotted η_{sp}/C and ln η_r/C against C for the data obtained by use of a capillary viscometer. For data of PVA solutions without SB, η_{sp}/C and ln η_r/C were each located on a straight line, so that intrinsic viscosity for solution without SB, $[\eta]_0$, was easily estimated. For the solution with SB, however, η_{sp}/C did not increase linearly with increasing C, and the slope increased with increasing C, as shown in Figure 3. It has been reported that the semilogarithmic plot of η_{sp}/C vs C gives the straight line for viscosity data of solutions of cellulose nitrate in ethyl acetate, poly(vinyl chloride) in dioxine, and so on.[13−15] When this type of plot was applied for viscosity data of PVA solutions with SB, all data for each PVA sample were located on a straight line. It should be noted that

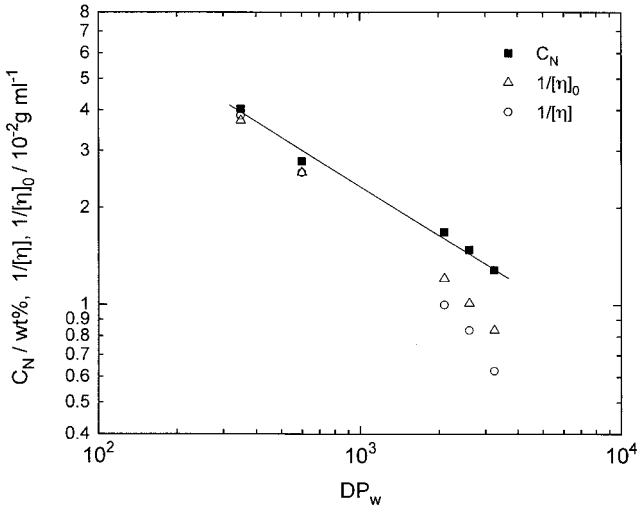

Figure 2. Molecular weight dependencies of C_N, $[\eta]_0$, and $[\eta]$ shown as a plot of C_N, $1/[\eta]_0$, and $1/[\eta]$ against DP_w. The units of wt % and 10^{-2} g mL^{-1} for the vertical axis could be regarded as approximately the same unit for our system, because the solution was aqueous one in low concentration range.

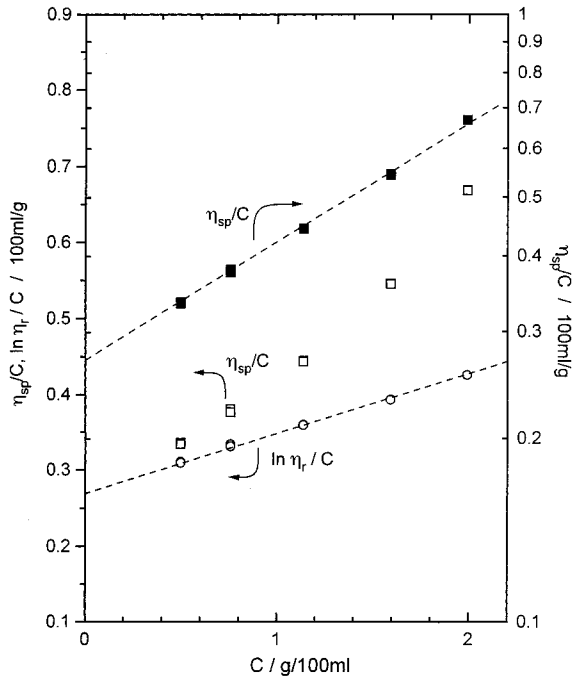

Figure 3. The η_{sp}/C and ln η_r/C are linearly plotted against C and η_{sp}/C is semilogarithmically plotted against C for the solution of PVA350 with SB.

the viscosity data for solution with higher C near and above C_N were not located on the straight line extrapolated to higher C but fairly above the line. We estimated intrinsic viscosity for solutions with SB, $[\eta]$, using two types of plot for η_{sp}/C and the linear plot for ln η_r/C, and found good agreement between them. The results are listed in Table 1. It should be noted that $[\eta]_0$ is estimated under the condition that the concentration of SB is half of that of PVA for all solutions.

Properties of Dynamic Viscoelasticity. The angular frequency, ω, dependence of the storage and loss moduli, G' and G'', for samples of PVA3250-2.0 and PVA350-5.0 are shown in Figure 4. The η and the mechanical relaxation time, τ_M, were estimated from the data in the fluid region, and the plateau modulus, G_N, was estimated from the data in the plateau region.

Table 1. Experimental Results of the PVA/SB Systems with $C > C_N$

sample	C_N/wt%	$[\eta]_0/10^2$ mL g^{-1} [a]	$[\eta]/10^2$ mL g^{-1} [b]
PVA350	4.02	0.27	0.26
PVA600	2.78	0.39	0.39
PVA2100	1.68	0.83	1.0
PVA2600	1.48	0.99	1.2
PVA3250	1.28	1.2	1.6

[a] PVA in aqueous solution without SB. [b] PVA in aqueous solution with SB.

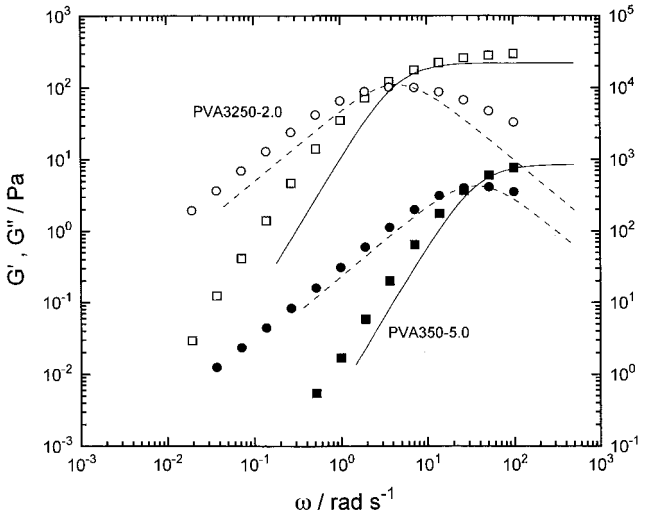

Figure 4. Angular frequency ω dependence of the storage and the loss moduli, $G'(\omega)$ and $G''(\omega)$, of two solutions whose DP_w and C are given in the figure. Solid and broken lines are fitting curves of $G'(\omega)$ and $G''(\omega)$ for PVA350-5.0 and PVA3250-2.0, respectively. The solid and broken lines are theoretical line of $G'(\omega)$ and $G''(\omega)$, respectively, for each solution assuming the Maxwell model with single relaxation time.

They are listed in the Tables 2 and 3.

Figure 5 shows the concentration dependence of G_N. G_N for the samples with different molecular weight increases concavely to the horizontal axis. There seems a possibility that one composite curve may be obtained by reducing G_N and C using proper values.

In the previous paper,[2] we reported the good agreement between the mechanical relaxation time, τ_M, and the characteristic time, τ_s, of the slow mode determined by DLS measurement, that is, the presence of the dynamical coupling between concentration fluctuation and elastic stress of the network. The agreement of τ_M with τ_s was also observed for the samples with DP_w of 350 and 3250 as shown in Figure 6. The τ_M and τ_s increase with increasing C concavely to the horizontal axis in lower C region, but they appear to be starting to curve upward with C for higher DP_w in high C region.

The ω dependencies of G' and G'' for the solutions with C near C_N are similar to those given by the Maxwell model with a single relaxation time. But the applicability became worse with increasing C. If the Maxwell model with a single relaxation time is satisfied, the relaxation time, τ_M', may be related with η and G_N as $\tau_M' = \eta/G_N$. Therefore, when the model is perfectly applicable to the data, then τ_M/τ_M' is unity, which is one of measures for applicability of the model to the experimental data and is listed in Table 4. The τ_M/τ_M' value tends to increase with increasing C. The values for most of the solutions measured are around 2 or less, which indicates that the Maxwell approximation is fairly good. However, solutions with high C and high M have larger

Table 2. Experimental Results of the PVA/SB System with $DP_w = 3250$

sample code	C/wt %	pH	$D_c/10^{-7}$ cm^2 s^{-1}	ξ_H/nm	τ_s/s	τ_M/s	G_N/Pa	$D_s/10^{-8}$ cm^2 s^{-1}	R_s/nm	η/Pa	$A_s/(A_f + A_s)$
PVA3250-1.0	1.0	8.8	5.3 ± 0.2	4.6 ± 0.2				30 ± 4		0.01 ± 0.001	
PVA3250-1.1	1.1	8.9	5.3 ± 0.2	4.6 ± 0.2				6.4 ± 0.5	33	0.018 ± 0.002	
PVA3250-1.2	1.2	8.9	5.2 ± 0.2	4.7 ± 0.2				2.1 ± 0.3	70	0.069 ± 0.004	
PVA3250-1.3	1.3	8.9	4.7 ± 0.3	5.2 ± 0.5	0.074 ± 0.2	0.075 ± 0.028				0.37 ± 0.03	0.22 ± 0.03
PVA3250-1.4	1.4	8.8	4.8 ± 0.2	5.1 ± 0.3	0.077 ± 0.025	0.089 ± 0.041	20 ± 2			1.7 ± 0.4	0.24 ± 0.05
PVA3250-1.5	1.5	8.8	4.9 ± 0.2	5.0 ± 0.3	0.19 ± 0.06	0.18 ± 0.03	40 ± 3			4.8 ± 0.6	0.27 ± 0.03
PVA3250-1.7	1.7	8.7	5.2 ± 0.2	4.7 ± 0.2	0.34 ± 0.13	0.4 ± 0.03	130 ± 10			26 ± 3	0.31 ± 0.05
PVA3250-2.0	2.0	8.8	5.6 ± 0.3	4.4 ± 0.2	0.72 ± 0.16	0.75 ± 0.16	330 ± 40			108 ± 14	0.40 ± 0.04
PVA3250-2.5	2.5	8.6	6.0 ± 0.3	4.1 ± 0.2	1.6 ± 0.5	1.8 ± 0.8	1100 ± 60			550 ± 24	0.46 ± 0.04
PVA3250-3.0	3.0	8.7	6.4 ± 0.3	3.8 ± 0.2	5.6 ± 1.5	5.7 ± 1.4	2400 ± 170			2050 ± 160	0.56 ± 0.05

Table 3. Experimental Results of the PVA/SB System with $DP_w = 350$

sample code	C/wt %	pH	$D_c/10^{-7}$ cm^2 s^{-1}	ξ_H/nm	τ_s/s	τ_M/s	G_N/Pa	$D_s/10^{-8}$ cm^2 s^{-1}	R_s/nm	η/Pa	$A_s/(A_f + A_s)$
PVA350-3.0	3.0	8.7	9.8 ± 0.2	2.5 ± 0.1				2.7 ± 0.6	23	0.0063 ± 0.0003	
PVA350-3.4	3.4	8.9	9.8 ± 0.4	2.5 ± 0.2				1.1 ± 0.2	30	0.013 ± 0.002	
PVA350-3.6	3.6	8.8	9.4 ± 0.4	2.6 ± 0.2				0.51 ± 0.05	40	0.027 ± 0.002	
PVA350-3.8	3.8	8.8	9.4 ± 0.4	2.6 ± 0.2				0.19 ± 0.02	55	0.072 ± 0.002	
PVA350-4.0	4.0	8.7	9.8 ± 0.3	2.5 ± 0.2				0.12 ± 0.03	60	0.23 ± 0.01	
PVA350-4.5	3.5	8.9	7.7 ± 0.3	3.2 ± 0.2	0.029 ± 0.011	0.025 ± 0.004				5.2 ± 0.2	0.46 ± 0.03
PVA350-5.0	5.0	8.7	8.4 ± 0.3	2.9 ± 0.1	0.036 ± 0.014	0.037 ± 0.006	910 ± 100			31 ± 4	0.54 ± 0.04
PVA350-6.0	6.0	8.5	8.8 ± 0.5	2.8 ± 0.4	0.066 ± 0.024	0.064 ± 0.007	3500 ± 350			154 ± 16	0.56 ± 0.04
PVA350-7.0	7.0	8.6	8.8 ± 0.4	2.8 ± 0.2	0.1 ± 0.02	0.1 ± 0.01	8200 ± 900			415 ± 35	0.73 ± 0.02

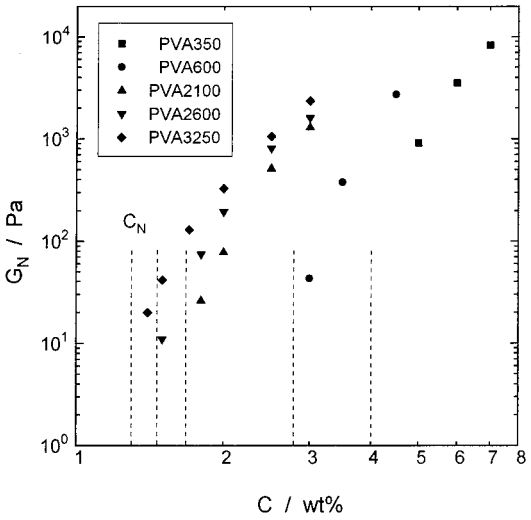

Figure 5. C dependence of the plateau modulus G_N for five PVA samples. The broken line for each sample indicates C_N.

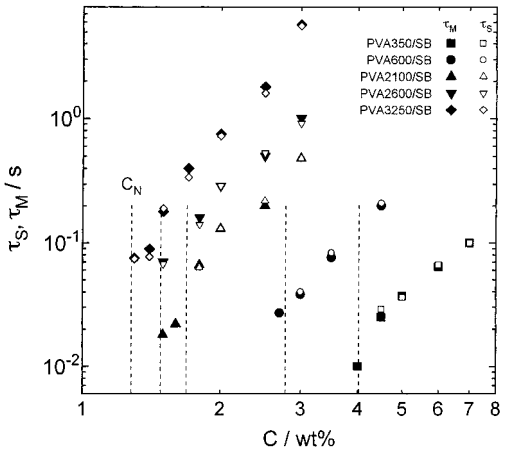

Figure 6. The mechanical relaxation time, τ_M, and the characteristic time, τ_s, of the slow mode above C_N, indicated as a broken line for each sample, are compared. The τ_M values of four solutions below C_N are also shown in the figure.

values for τ_M/τ_M', e.g. 3.4 for PVA3250-2.5 and 6.7 for PVA3250-3.0. Actually, the theoretical curve expected from the single Maxwell type of the model was not in agreement with the experimental data for these solutions.

One of the reasons for the deviation is the entanglement effect. The dynamic viscoelastic measurement showed that even a solution without SB having the highest C and DP values of the PVA sample, i.e. PVA3250-3.0 without SB, had a terminal relaxation time much shorter than 10^{-2} s. Therefore, the terminal relaxation time is shorter than τ_M of the solution with SB by at least 2 or 3 orders of magnitude, which means that the entanglement effect is not a dominant factor for the deviation of the experimental results from the model.

The longest relaxation time, τ_1, of the Rouse model for dilute to semidilute solution is given by the following equation[16]

$$\tau_1 = 6(\eta - \eta_s)M/\pi^2 CRT \qquad (1)$$

where R is gas constant and T the absolute temperature. We found that τ_M disagreed with τ_M' when τ_1 was comparable with τ_M. The τ_1 is the time required for relaxation of not a part of the chain but the whole chain. Consequently, we propose the following picture. A PVA chain almost always is confined in the network by several complexes with a finite lifetime. Once the confinement of the PVA chain is released by the dissociation of the complex, then the conformational relaxation occurs. For the solution with low C and with low M, the time for relaxation of the whole chain is shorter than the time for reassociation with the network; thus, the stress in the chain may be relaxed thoroughly for the whole chain. Therefore, the relaxation time is determined mainly by the lifetime of crosslinks which sustain applied stress. On the other hand, for the solution with high C and high M, the releasing time is not long enough for the PVA chain to relax its deformed conformation; therefore, it takes longer for the applied stress for whole system to relax. So the single Maxwell model is no longer satisfied.

DLS Behavior. In this section, we describe DLS results which emphasize the important role of C_N for

Table 4. Experimental Results of the PVA/SB Systems with $C > C_N$

sample code	C/wt %	C/C_N	τ_M/s	G_N/Pa	η/Pa s	τ_M'/s	τ_1/s	τ_M/τ_M'	τ_M/τ_1	$\nu_{eff}/10^{23}$ m^{-3}	$\nu/10^{23}$ m^{-3}	ν_{eff}/ν
PVA3250-1.4	1.4	1.09	0.089	20	1.7	0.085	0.00475	1.0	18.7	0.58	5.3	0.11
PVA3250-1.5	1.5	1.17	0.18	40	4.8	0.120	0.0125	1.5	14.4	1.2	5.7	0.20
PVA3250-1.7	1.7	1.33	0.4	130	26	0.20	0.0598	2.0	6.7	3.8	6.4	0.59
PVA3250-2.0	2.0	1.56	0.75	330	108	0.33	0.211	2.3	3.6	9.6	7.6	1.3
PVA3250-2.5	2.5	1.95	1.8	1100	550	0.50	0.861	3.6	2.1	32	9.5	3.4
PVA3250-3.0	3.0	2.34	5.7	2400	2050	0.85	2.67	6.7	2.1	70	11	6.1
PVA2600-1.5	1.5	1.01	0.07	11	0.5	0.0455	0.00104	1.5	67.1	0.32	7.1	0.045
PVA2600-1.8	1.8	1.22	0.16	75	9.2	0.123	0.0160	1.3	10.0	2.2	8.5	0.26
PVA2600-2.0	2.0	1.35	0.29	200	35	0.175	0.0548	1.7	5.3	5.8	9.5	0.61
PVA2600-2.5	2.5	1.69	0.5	800	260	0.33	0.325	1.5	1.5	23	12	2.0
PVA2600-3.0	3.0	2.03	1	1600	650	0.41	0.678	2.5	1.5	46	14	3.3
PVA2100-1.8	1.8	1.07	0.066	26	1.0	0.0385	0.00140	1.7	47.0	0.75	11	0.072
PVA2100-2.0	2.0	1.19	0.13	78	6.5	0.0833	0.00821	1.6	15.8	2.3	12	0.19
PVA2100-2.5	2.5	1.49	0.2	500	65	0.130	0.0657	1.5	3.0	14	15	0.99
PVA2100-3.0	3.0	1.79	0.48	1300	300	0.23	0.253	2.0	1.9	38	18	2.1
PVA600-3.0	3.0	1.08	0.038	43	0.9	0.0209	0.00022	1.8	175.4	1.2	61	0.020
PVA600-3.5	3.5	1.26	0.076	380	15	0.0395	0.00309	1.9	24.6	11	72	0.15
PVA600-4.5	4.5	1.62	0.2	2700	270	0.100	0.0433	2.0	4.6	78	92	0.85
PVA350-4.5	4.5	1.12	0.025		5.2		0.00049		51.4		158	
PVA350-5.0	5.0	1.24	0.037	910	31	0.0341	0.00261	1.1	14.2	26	176	0.15
PVA350-6.0	6.0	1.49	0.064	3500	154	0.044	0.0108	1.5	5.9	101	211	0.48
PVA350-7.0	7.0	1.74	0.1	8200	415	0.0506	0.0250	2.0	4.0	237	246	0.97

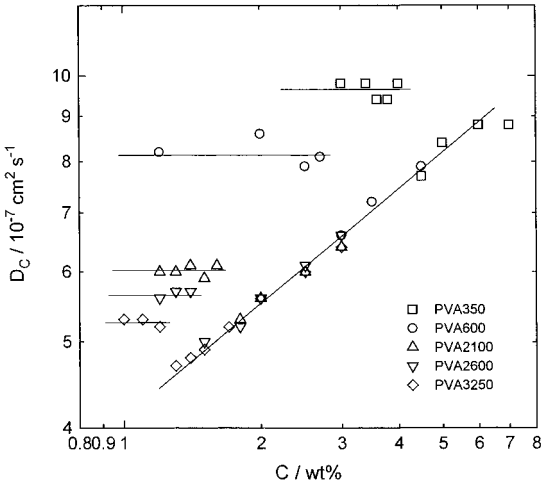

Figure 7. Plot of the cooperative diffusion coefficient D_C corresponding to the fast mode against C. The C and M dependencies of D_C are utterly different between the regions above and below some critical concentration C_N dependent PVA molecular weight.

the concentration fluctuation dynamics of PVA/SB solution. Normalized time correlation function, $A_q(t)$, of scattered light intensity revealed that the solutions possess two dominant decaying modes, fast and slow, with the decay rates of Γ_f and Γ_s ($\Gamma_f < \Gamma_s$), respectively. Analysis of the slow and fast modes showed that the decaying behavior of $A_q(t)$ was entirely divided into two groups below and above a critical concentration, being in good agreement with C_N defined by the C dependence of $\eta - \eta_s$.

Γ_f corresponding to the fast mode was proportional to q^2 for all solutions, where q is the magnitude of the scattering vector defined by $q = (4\pi/\lambda)\sin(\theta/2)$, where λ is the wavelength in the medium. This result indicates that the fast decaying mode is the diffusive one. The cooperative diffusion coefficient, D_C, could be evaluated as an average of Γ_f/q^2 and plotted against C in Figure 7, which shows that C and M dependencies of D_C are utterly different in the two regimes above and below C_N, where D_C abruptly changes with change of C. The D_C depends on M but is independent of C in the lower C region, whereas it becomes independent of M but increases with increasing C in the higher C region. We estimated the dynamic correlation length, ξ_H, from D_C using the Einstein−Stokes relationship $\xi_H = k_B T/6\eta_s D_C$, where k_B is the Boltzman constant. We could determine the relation of ξ_H with M and C as follows:

$$\xi_H \sim C^0 M^{0.25\pm0.03}, \quad C < C_N \tag{2}$$

$$\xi_H \sim C^{-0.42\pm0.02} M^0, \quad C > C_N \tag{3}$$

The q dependence of the decay rate Γ_s corresponding to the slow mode was quite different between the two regions below and above C_N. In the region below C_N, Γ_s/q^2 appears almost independent of q, which indicates that this mode is the diffusive one. As C increases toward C_N, Γ_s/q^2 still remains constant at low q but starts to increase with q at high q. The slope asymptotically becomes unity at high q at C close to C_N in a logarithmic plot of Γ_s/q^2 against q. In Tables 2 and 3, we listed the characteristic quantity D_s estimated as the value of Γ_s/q^2 linearly extrapolated to $q = 0$. We found applicability of the dynamic scaling theory[17] to data of Γ_s for three PVA samples with $DP_w = 600$, 2100, and 2600 in a previous paper,[2] i.e., the reduced plot of $\Gamma_s/D_s q^2$ against qR_s were well superposed on a master curve representing the Kawasaki function.[18] In the procedure, we used R_s as a fitting parameter. The applicability was also satisfied for the samples with $DP_w = 350$ and 3250. Estimated values of R_s are listed in Tables 2 and 3. Such a q dependence of Γ_s/q^2 shows that the observed slow mode originated from translational diffusion of the clusters, i.e. aggregate of PVA chains, with the size around R_s at lower q and from the internal motion of cluster due to the consecutive association−dissociation process of the complexes at higher q at C near but lower than C_N. If it is the case, fairly large clusters with diameter of almost 100 nm should be formed near C_N in the region of $C < C_N$.

In a region of $C > C_N$, Γ_s was independent of q over the whole range of the scattering angle from 15° to 150° measured, which indicates that this is the structural relaxation mode. Values of the characteristic time, τ_s, were calculated as the reciprocal of averaged Γ_s and are listed in Tables 2 and 3. This mode should come from the relaxation process due to the consecutive association−dissociation process of the complex as temporal

cross-links in the network as revealed by good agreement between τ_s and τ_M.

Discussion

Behavior of Dilute Solution. According to the scaling concept developed by de Gennes,[4] the characteristic length scale of a solution of neutral polymers in the dilute region is the radius of gyration, R_G, or hydrodynamic radius, R_H, which corresponds to the chain dimension of polymer in solution. On the other hand, the C dependence of viscosity in this regime was experimentally well-established as the Huggins relationship, which relates reduced viscosity η_{sp}/C of a polymer solution to intrinsic viscosity, $[\eta]$[19]

$$\eta_{sp}/C = [\eta] + k'[\eta]^2C + ... \quad (4)$$

where k' is the Huggins constant. The equation suggests that $\eta - \eta_s$ is expressed by a function of $C[\eta]$ and that C dependence of viscosity of polymer solution in low C range may be represented by a reduced curve using $C[\eta]$ regardless of its molecular weight. When we remember that $[\eta]$ is related to R_G, R_H, and M as $[\eta] \sim R_G^2R_H/M$ using the characteristic length scales R_G and R_H and means the occupied volume of chain per weight, the Huggins relationship may be regarded as one of the applications of the scaling concept to viscosity using a perturbed approximation.

The $[\eta]_0$ and $[\eta]$ listed in Table 1 are shown in Figure 2 as plots of $1/[\eta]_0$ and $1/[\eta]$ against DP_w. The slope of $1/[\eta]_0$ appears close to $-1/2$ in the low DP_w region and decreases with increasing DP. This may indicate that the usual excluded volume effect by contact between chains is almost negligible for the sample with the lowest DP_w and makes the chain dimension larger for sample with the higher DP. On comparison of the intrinsic viscosities of PVA solutions with and without SB, they have almost the same value for samples with lower DP_w of 350 and 600. For samples with higher DP, on the other hand, addition of SB to PVA solution makes $[\eta]$ larger and the difference increases with increasing DP. The deviation may be ascribed to an association effect between chains and also to a polyelectrolyte effect by formation of ionic complex formation.[20,21] At least, the similar values of $[\eta]$ and $[\eta]_0$ for samples with lower DP indicate that chain conformation for lower DP is not affected by such effects. Therefore, the sample with lower DP such as PVA350 should possess the unperturbed dimension, while for the sample with the higher DP both the usual excluded volume and the complex formation effects make the chain dimension larger.

We tried to superpose viscosities of the solutions of PVA/SB system by use of $C[\eta]$ as the horizontal axis in Figure 8 in order to check the applicability of the Huggins relationship to our data. The C dependence of viscosity is fairly well represented by one curve in the lower C region, and the Huggins relationship is practically satisfied in the region $C[\eta] < 0.2$, while data near and above C_N are not located on one composite curve at all. It should be noted that if the logarithm of η_{sp}/C is actually proportional to C in the low C region as described in the Results section, the Huggins relationship is not strictly satisfied. This feature may be possibly one of the general features of solutions of associating polymers because several associating polymers also exhibit the same tendency as mentioned in the Results section.

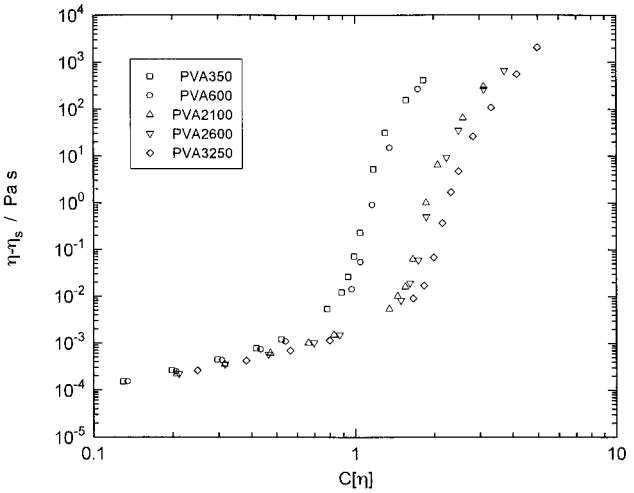

Figure 8. Attempt to superpose the viscosity by reducing C by $1/[\eta]$ in the plot of $\eta - \eta_s$. In the lower C region, the superposition looks good, but in the higher C region, the data are not well superposed.

As described above, the chain dimension of polymers was expanded from the unperturbed state in the low C region due to the effects of the complex formation such as the polyelectrolyte effect and association effect. The extent of the effects should change with changing C. Thus the chain dimension around C_N should be different from that in the low C region. Suppose that the effects of contraction and expansion cancel each other and that the property of the chain around C_N approaches that in swollen gel exhibiting Gaussian behavior, then it can be assumed that the chain dimension around C_N might be related with DP as $[\eta]_{up} \sim DP^{1/2}$, where $[\eta]_{up}$ denotes the chain dimension per molecular weight for solution around C_N with unperturbed dimension. The subscript up denotes the unperterbed state. Because the chain dimension of PVA350 is not affected very much by the effects of complex formation even in dilute solution, $[\eta]_{up}$ should be almost same as $[\eta]$ for PVA350. Therefore, we may estimate $[\eta]_{up}$ for the other samples using $[\eta]_{up}$ for PVA350 as standard. Further, we may obtain overlapping concentration around C_N, C^*_{up}, by $C^*_{up} = 1/[\eta]_{up}$. We made a plot of $\eta - \eta_s$ against C/C^*_{up} in Figure 9, where all data around $C = C_N$ are fairly well represented by one sigmoidal curve. It should be remarked that all inflection points are located around $C/C^*_{up} = 1$. These results give us one of the simplest idea for the physical meaning of C_N: C_N corresponds to the overlapping concentration for the unperturbed PVA chain. The molecular weight distribution of our samples are fairly broad, so we need the more precise experiment using the monodisperse samples in order to conclude it definitely. However, the DP dependence of C_N could be expressed by the relation $C_N \sim DP^{-0.53}$, which is in good agreement with the idea.

Elastically Effective Chain. Observation of the plateau for the storage shear modulus in dynamic viscoelastic measurements indicates that the dissociation−association process of complexes, i.e., rearrangement of network, does not take place in such a short time region so that the transient network may be regarded as a gel with permanent cross-links. In this case, we may evaluate the number of elastically effective chains ν_{eff} using $G_N = \nu_{eff}k_BT$. In a previous paper,[3] we interpreted the C dependence of G_N using the theory of rubberlike elasticity and the density of elastically ef-

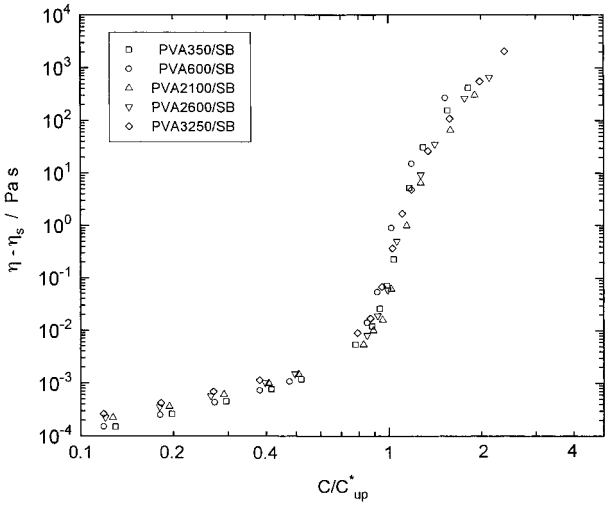

Figure 9. Plot of η-η_s against C/C^*_{up}, where C^*_{up} is defined by $C^*_{up} = 1/[\eta]_{up}$. $[\eta]_{up}$ is estimated using the $[\eta]$ of PVA350 as a standard on the assumption that the polymer behaves as a Gaussian chain. The subscript up means the unperturbed state.

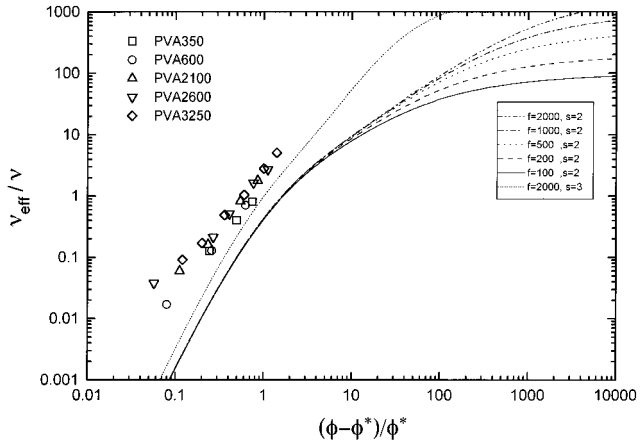

Figure 10. Plot of ν_{eff}/ν against $(\phi - \phi^*)/\phi^*$. Each line presents a theoretical prediction for each condition with functionality f and multiplicity s. Experimenatal data are also plotted using $(C - C_N)/C_N$ as horizontal axis, where the weight average molecular weight values were used for the estimation of ν.

fective chains estimated from ξ_H. On the other hand, if we could regard the phenomenon of increase in G_N with increasing C as the gelation and network growth process, C_N might be taken as the sol−gel transition point. Then the G_N data may be interpreted using a statistical−mechanical theory for elastically effective chain in transient gels developed by Tanaka and Ishida[6] quite recently.

The network is modeled as a collection of primary flexible chains with n repeated units carrying f functional groups capable of forming multiple junctions, each of which is composed of m functional groups combining more than two chains. In the theory, they used mean-field approximation to specify a process of network growth that is essentially the same method as Flory's tree model,[22] and they adopted the Scanlan−Case criterion[23,24] for a chain to be elastically effective, which proposes that chains connected at both ends to junctions with at least three paths to the gel network are elastically effective. The theory allows us to evaluate the ratio of the number density of elastically effective chain, ν_{eff}, and the number density of primary chain (or polymer chain), ν, as a function of a scaled concentration, $\lambda\phi f/n$, where ϕ is the volume fraction of polymer and λ the association constant which is related to the reaction constant of junctions.

In the PVA/SB system, two successive monomers with two hydroxy groups can play the role of a functional group. Thus, we may assume that f is proportional to DP and m is equal to 2. In this case, the theory predicts that ν_{eff}/ν increases with increasing $\lambda\phi f/n$ and approaches to $f - 1$ as $\lambda\phi f/n$ approaches infinity. On the other hand, ν_{eff}/ν becomes 0 with $\lambda\phi f/n$ of $(f - 1)/(f - 2)^2$, which is a critical point of the sol−gel transition. The ϕ corresponding to this point is denoted by ϕ^*. If we take $\lambda\phi^* f/n$ as a standard point of the scaled concentration and assume that λ is independent of concentration of chain, we may plot ν_{eff}/ν against the reduced concentration $(\phi - \phi^*)/\phi^*$, as shown in Figure 10. The remarkable feature is that the $(\phi - \phi^*)/\phi^*$ dependence of ν_{eff}/ν is almost identical in the region of $(\phi - \phi^*)/\phi^* < 10$ for polymers with large f ($f > 100$). Thus we may regard the curve as a master curve of the dependence of ν_{eff}/ν for polymers with $f > 100$. The degree of saponification of our PVA samples was about 88 mol %, which means that 12 mol % of hydroxy groups still remain as actylated residues. An estimate of f as DP $\times$ 0.88^2 gives that the PVA sample with lowest DP of 350 has $f = 270$, being much larger than 100. It seems a good approximation that the volume fraction of polymer, ϕ, is almost proportional to C. The ν_{eff} and ν can be determined from experiment. Thus, when a critical concentration corresponding to ϕ^* is determined, we can compare the experimental data with the theoretical prediction without any fitting parameter in Figure 10. For the PVA/SB system, cluster formed by associating chains expanded to the whole system at C_N. The phenomenon is similar to the behavior of gel point for chemical gelation, where the cluster with infinite molecular weight is formed to expand to the whole system, which gives us an idea that C_N corresponds to the critical concentration ϕ^*. In Figure 10, experimental ν_{eff}/ν were plotted against $(C - C_N)/C_N$ as horizontal axis. Our sample had broad molecular weight distribution ($M_W/M_N > 2$). This distribution affects estimation of ν and, therefore, ν_{eff}/ν. It is well-known that the critical point of sol−gel transition is the point at which the weight-average molecular weight of cluster diverges. The degree of reaction of the functional group at the critical point, which determines the critical concentration, is then supposed to be determined by the weight-average functionality of the primary chains, f_W, proportional to DP_w.[25] It is difficult to say definitely what average molecular weight should be used to evaluate ν_{eff}/ν. Here, we calculated ν using the weight-average molecular weight.

As shown in Figure 10, all C dependence of ν_{eff}/ν for PVA samples with different molecular weight were superposed on a smooth curve, which indicates that this type of analysis is useful and we can compare the composite curve with the theoretical curve.

At a glance, the dependence of experimental ν_{eff}/ν on $(C - C_N)/C_N$ looks similar to the theoretical curve. Nevertheless, some discrepancies are observed between theory and experiment. One of them is the difference in slope in the low C region, where the experiment gives 1.5−2.0 and the theory gives 3. It is known that the slope in the low C region is very susceptible to the value of C_N. The C_N was defined by the inflection point of the plot of $\eta - \eta_s$ against C, which may include a small

extent of uncertainty. On the other hand, as DLS results showed a transition with C, we can determine the maximum and the minimum values of C for C_N among all C measured by DLS. It should be noted that, even if we take any value in the C range as C_N, the slope is always less than 2. The slope of 3 in the theoretical curve with decreasing $(\phi - \phi^*)/\phi^*$ is a general result coming from the mean-field treatment. The association probabilities between intra- and interchains is assumed to be the same in the mean-field treatment, while, in the actual system, they should be different, especially in the C region quite near C_N corresponding to the overlapping concentration. The inapplicability of the mean-field approximation to the network formation of samples should bring about the deviation between the experimental data and the theory. In the cases of the experimental data of chemical gel[9,26] and the theoretical prediction of the percolation theory,[4] the critical exponent is known to be around 1.8−2.0. Our data is rather close to these values.

When the probability of contact with another chains becomes higher with increasing C, the applicability of the mean-field model to the experimental system should become better. Especially the ability of cross-links to rearrange our system makes the applicability more reliable. Therefore, with increasing C, the C dependence of experimental ν_{eff}/ν must asymptotically approach to the theoretical curve. However, the absolute value does not approach to the theoretical one at all. Furthermore, neither does the slope. When we think about difference between the absolute value of ν_{eff}/ν, two possibilities may be listed for this deviation. One of the possibilities should arise from the theory in which the tree statistics were adopted in the same way as Flory's tree model,[22] where it is assumed that the sol fraction has no loop structure. The loop formation in sol fraction must occur in the actual system. Therefore, the hypothesis should not be satisfied, which may bring about the difference between the theoretical values and the experimental data. With increasing C, the effect may be neglected because the sol fraction becomes smaller. However, the deviation did not become small in higher C region. Therefore, the effect may be not enough to explain the deviation. Another possibility may come from the sample. The molecular weight distribution of our samples is fairly broad, which should influence the estimation of ν. If we adopted number-average molecular weight to calculate ν, which gave about twice as large a ν value as weight-average molecular weight, the data points became closer to the theoretical curve, but it was not enough for the data to be located on the theoretical curve. It should be remembered that there is no justification for using number-average molecular weight. Besides, it is difficult to evaluate easily from the theory how much the distribution changes ν_{eff}/ν now.

The second difference, i.e. that the asymptotically approaching behavior of the slope could not be observed in the higher C region, should be a serious problem when comparing the experimental data with theory, because all effects on the deviation described above except the polydispersity become negligible in the higher C region. The difference might imply that some of our assumptions on the comparison with theory should be incorrect. From the structure of the complex between the borax ion and hydroxy groups, we supposed that the multiplicity of the connection, m, is 2, i.e., pairwise junction. On the other hand, when 3 was adopted as m, the theoretical curve given in the dotted line was located quite near the experimental value, as shown in Figure 10, which may indicate the possibility of the existence of junction points in which more than three chains participate in. The characteristic relaxation time on the order of over 1 ms seems to be quite long as the lifetime of the didiol complex under equilibrium condition, which might come from this multiplicity. However, there are no data justifying the assumption now. If the multiple junction exists, the probability of occurrence of the junction should vary with the probability of existence of two successive hydroxy groups on a chain, i.e., the saponification of PVA samples. We are carrying out such experiments now.

Acknowledgment. The authors are grateful to Kuraray Co. Ltd. for a gift of PVA samples. We are indebted to Prof. F. Tanaka for valuable discussion.

References and Notes

(1) Koike, A.; Nemoto, N.; Inoue, T.; Osaki, K. *Macromolecules* **1995**, *28*, 2339.
(2) Nemoto, N.; Koike, A.; Osaki, K. *Macromolecules* **1996**, *29*, 1445.
(3) Takada, A.; Nemoto, N. *Progress Colloid Polym. Sci.* In press.
(4) de Gennes, P.-G. *Scaling Concepts in Polymer Physics*; Cornell University Press: Ithaca, NY, 1979.
(5) Matumoto, M.; Ohyanagi, Y. *Koubunshi Kagaku* **1960**, *17*, 191 (in Japanese).
(6) Tanaka, F.; Ishida, M. *Macromolecules* **1996**, *29*, 7571.
(7) Chanbon, F.; Winter, H. H. *Polym. Bull.* **1985**, *13*, 499.
(8) Winter, H. H.; Chambon, F. *J. Rheol.* **1986**, *30*, 367.
(9) Koike, A.; Nemoto, N.; Takahashi, M.; Osaki, K. *Polymer* **1994**, *35*, 3005.
(10) Hossain, K. S.; Nemoto, N.; Nishinari, K. *Nihon Reoroji Gakkaishi* In press.
(11) Maerker, J. M.; Sinton, S. W. *J. Rheol.* **1986**, *30*, 77.
(12) Osaki, K.; Inoue, T.; Ahn, K. H. *J. Non-Newtonian Fluid Mech.* **1994**, *54*, 109.
(13) Spurlin, H. M.; Martin, A. F. *J. Polym. Sci.* **1946**, *1*, 63.
(14) Ott, E.; Spurlin, H. M.; Grafflin, M. W., Eds, *Cellulose and Cellulose Derivatives*, Interscience Publishers, 1955; Part III, pp 1189, 1203.
(15) Nakajima, A. *Koubunshi Kagaku* **1950**, *7*, 309 (in Japanese).
(16) Ferry, J. D. *Viscoelastic Properties of Polymers*; John Wiley: New York, 1980.
(17) Doi, M.; Edwards, S. F. *The Theory of Polymer Dynamics*; Oxford University Press: Oxford, 1986.
(18) Kawasaki, K. In *Critical Phenomena*; Green, M. S., Ed.; Academic Press: New York, 1971; p 342.
(19) Huggins, M. L. *J. Am. Chem. Soc.* **1943**, *64*, 2712.
(20) Ochiai, H.; Kurita, Y.; Murakami, I. *Makromol. Chem.* **1984**, *185*, 167.
(21) Shibayama, M.; Uesaka, M.; Inamoto, S.; Mihara, H.; Nomura, S. *Macromolecules*, **1996**, *29*, 885.
(22) Flory, P. J. *Principles of Polymer Chemistry*; Cornell University Press: Ithaca, NY, 1953; Chapter 3.
(23) Scanlan, J. *J. Polym. Sci.* **1960**, *43*, 501.
(24) Case, L. C. *J. Polym. Sci.* **1960**, *45*, 397.
(25) Fukui, K.; Yamabe, T. *Bull. Chem. Soc. Jpn.* **1967**, *40*, 2052.
(26) Peniche-Covacs, C.; Dev, S.; Gordon, M.; Judd, M.; Kajiwara, K. *Polymer Networks*, Chompff, M; Newman, S. Eds.; Plenum Press: New York, 1971.

MA970859+